Theor Chem Acc (2011) 130:633–644
DOI 10.1007/s00214-011-1007-8

REGULAR ARTICLE

An improved algorithm for the normalized elimination of the small-component method

Wenli Zou · Michael Filatov · Dieter Cremer

Received: 7 April 2011 / Accepted: 14 July 2011 / Published online: 27 August 2011

Abstract A new algorithm for the iterative solution of the normalized elimination of the small component (NESC) method is presented that is less costly than previous algorithms and that is based on (1) solving the NESC equations for the uncontracted rather than contracted basis ("First-Diagonalize-then-Contract"), (2) a new iterative procedure for obtaining the NESC Hamiltonian ("iterative TU algorithm"), (3) the renormalization scheme connected to the picture change, and (4) a finite nucleus model with a Gaussian charge distribution. The accuracy of NESC energies, which match those of 4-component Dirac calculations, is demonstrated. Test calculations with CCSD(T), DFT, and large basis sets including high angular momentum basis functions (f,g,h,i) are presented to prove the general applicability of the new NESC algorithm. Comparison with other algorithms of solving the NESC equations are shortly discussed and time savings are presented.

Keywords Normalized Elimination of the Small Component (NESC) · Exact quasi-relativistic methods · Picture change · Finite nucleus model

Dedicated to Professor Akira Imamura on the occasion of his 77th birthday and published as part of the Imamura Festschrift Issue.

W. Zou · D. Cremer (✉)
Department of Chemistry, Southern Methodist University, 3215 Daniel Ave, Dallas, TX 75275-0314, USA
e-mail: dcremer@smu.edu

M. Filatov
University of Groningen, 9747 AG Groningen, The Netherlands

1 Introduction

One of the primary objectives of current relativistic quantum chemistry is to transform the four-component (4c) Dirac equation [1, 2] into an exact, but nevertheless feasible and generally applicable two-component (2c) quasi-relativistic description of atoms and molecules. The purpose of such a transformation is to eliminate the (negative-energy) positron states because a description of positrons is chemically not interesting and leads only to computational difficulties and increased cost by treating a double set of (electronic and positronic) eigenstates. For the investigation of the majority of all chemical problems not involving a magnetic field, one needs only the (positive-energy) electronic states, which are dominated by the large component of the Dirac wavefunction [3–5]. For a free electron, this can be exactly done applying the Foldy-Wouthuysen (FW) transformation [6]. For bound electrons in atoms or molecules, the FW transformation is not available in closed algebraic form and therefore has to be approximated or replaced by other techniques where in the 1980s and 1990s perturbation was preferentially used. Best known is the Douglas–Kroll–Hess (DKH) method that has been worked out for low orders of n [7, 8–11] as well as higher orders [12, 13]. In the last years, infinite-order DKHn theory has been developed, which reproduces exact 4c-Dirac energies [14–18]. It has to be mentioned that DKHn theory suffers from its slow convergence and difficulties when formulating higher orders of the DKHn perturbation approach. Infinite-order theory offers in this regard an important improvement of DKH.

Much faster convergence is provided by the perturbation approach based on the regular approximation (RA) to the relativistic Hamiltonian [19]. However, the RA suffers from several technical problems and originally only ZORA

(zeroth-order regular approximation) [20] and IORA (infinite-order regular approximation; IORA is still a zeroth-order approach, however the relativistic normalization of the wave function is carried out at infinite order) [21] were developed where especially the Baerends group played an important role [22, 23]. Some of the obstacles of the RA were overcome by Filatov and Cremer by developing matrix representations of the ZORA and IORA Hamiltonians [24–27], deriving their relationship to an exact quasi-relativistic Hamiltonian [28] and solving the gauge-dependence problem of ZORA and IORA [29]. Although only low-order RA was implemented, the RA methods had an important impact on the improvement of the normalized elimination of the small component (NESC) method [28, 30].

A variational approach to the problem of obtaining an exact quasi-relativistic 2c-solution was formulated by Dyall in the form of the NESC method [31, 32]. NESC is a first principles 2c-approach in which the small component of the electronic wavefunction is eliminated using the restricted kinetic balance (RKB) prescription [33, 34]. In view of the fact that NESC provides the exact 2c relativistic description of one-electron systems, it can be used as an appropriate reference for approximate quasi-relativistic theories such as the RA or finite-order DKH methods. For some time, these possibilities could not be exploited because of the computational difficulties accompanying the solution of the NESC equations. A number of approximate NESC methods were suggested ranging from the atom-centered approximation of NESC developed by Dyall and Enevoldsen [35] to the low-order NESC approximations of Filatov and Cremer [36, 37]. A breakthrough was the work by Filatov and Dyall who presented for the first time a computationally feasible way of solving the NESC equations [38].

There have been a number of other approximate quasi-relativistic methods [39, 40] where we mention here just the infinite-order two-component (IOTC) relativistic Hamiltonian approach connecting to the original work of Barysz, Sadlej, and Snijders [41], which triggered a number of developments based on this approach [42–47]. Common to most of these developments is the fact that approximate 2c-Hamiltonians are derived at the operator level whereas the matrix representation of the final operator is obtained at a later stage. However, this procedure can be substantially simplified by starting with the matrix representation of the Dirac Hamiltonian in a finite basis set and then using matrix algebra to obtain a simplified relativistic Hamiltonian.

Dyall was the first who successfully applied such a matrix-driven approach when deriving NESC [31]. Iliaš et al. [48] also used matrix algebra to derive the IOTC Hamiltonian, which has led to substantial improvements of IOTC by Iliaš and Saue [49] and Barysz et al. [47], showing that IOTC can also provide exact quasi-relativistic values. Kutzelnigg and Liu have classified quasi-relativistic methods as being operator based or matrix based and pointed out in this connection that the latter lead much easier to an exact quasi-relativistic presentation of 4c-Dirac theory [50–52]. These authors describe the basic requirements for exact quasi-relativistic 2c (X2C or XQC) methods [53]. They identify NESC as X2C method, criticize however [54] the unnormalized version of NESC (UESC) also discussed in Dyall's original NESC paper [31]. This is in so far relevant as ZORA can be considered as a UESC-ZORA method and IORA as a NESC-ZORA method, as was pointed out by Filatov and Cremer [30]. Filatov [55] has emphasized that Dyall's NESC method [31] fulfills the criteria of exact X2C methods and therefore its practical realization [38] made X2C calculations generally available.

Previously, we have pointed out the relationship between IORA and NESC [30], which makes IORA a convenient starting point for an iterative solution of the NESC equations [38]. In this work, we present further improvements of NESC where we focus on both the accuracy of solving the NESC equations and the computational cost of NESC. In this connection, we will introduce a different strategy of setting up the NESC equations. In addition, we will combine NESC with a finite nuclear model and document the energy changes caused by this. Finally, we will demonstrate the effect of employing basis sets with high angular momentum functions in the case of NESC calculations. Test calculations will be carried out for mercury and thallium molecules.

This work is part of a larger research effort that involves the improvement of existing NESC algorithms and programs (the current paper), the derivation of analytical first-order energy derivatives to carry out NESC geometry optimizations [56], and the development of analytical second-order NESC derivatives (in progress) for calculating vibrational frequencies especially in connection with the URVA (unified reaction valley approach) analysis of the mechanism of chemical reactions as described by the reaction path curvature and the curvature coupling coefficients [37, 58]. These studies involve the repeated calculation of energy and its first and second derivatives along the reaction path at the NESC/DFT, NESC/MP2, etc. level of theory and thereby require an efficient solution of the NESC equation. Apart from this, the current work is the basis for calculating relativistic corrections in connection with the determination of first- and second-order response properties. In view of these objectives, we want to present NESC in this work as a feasible, generally applicable, and accurate quasi-relativistic method.

This article is organized as follows: In Sect. 2, the theoretical basis for the improvement of NESC is presented. Section 3 gives details of the calculations presented in Sect. 4. These calculations will show that NESC can compete with regard to its cost requirements with approximate quasi-relativistic methods.

2 Theory

Starting from the 4-component matrix Dirac equation [1, 2] with embedded restricted kinetic balance (RKB)

$$P\begin{pmatrix}\mathbf{V} & \mathbf{T}\\ \mathbf{T} & \mathbf{W}-\mathbf{T}\end{pmatrix}\begin{pmatrix}\mathbf{A}_p & \mathbf{A}\\ \mathbf{B}_p & \mathbf{B}\end{pmatrix} = \begin{pmatrix}\mathbf{S} & \mathbf{0}\\ \mathbf{0} & (2\mathrm{mc}^2)^{-1}\mathbf{T}\end{pmatrix}\begin{pmatrix}\mathbf{A}_p & \mathbf{A}\\ \mathbf{B}_p & \mathbf{B}\end{pmatrix}\begin{pmatrix}\mathbf{E}_p & \mathbf{0}\\ \mathbf{0} & \mathbf{E}\end{pmatrix}. \quad (1)$$

Dyall decoupled the positronic states with energies $\mathbf{E}_p$ and eigenvectors $\mathbf{A}_p$ and $\mathbf{B}_p$, respectively, and eliminated the small component with the help of the pseudo-large component represented by eigenvector matrix $\mathbf{B}$. Matrix $\mathbf{B}$ is related to the large component $\mathbf{A}$ via the matrix $\mathbf{U}$ as shown in Eq. 2 [31].

$$\mathbf{B} = \mathbf{UA} \quad (2)$$

This led to a simple eigenvalue equation (the NESC equation)

$$\tilde{\mathbf{L}}\mathbf{A} = \tilde{\mathbf{S}}\mathbf{A}\boldsymbol{\varepsilon} \quad (3)$$

for obtaining the large component $\mathbf{A}$ of the electronic relativistic wavefunction. The latter is normalized on the relativistic metric $\tilde{\mathbf{S}}$

$$\tilde{\mathbf{S}} = \mathbf{S} + \frac{1}{2\mathrm{mc}^2}\mathbf{U}^\dagger\mathbf{TU} \quad (4)$$

as $\mathbf{A}^\dagger\tilde{\mathbf{S}}\mathbf{A} = \mathbf{I}$, which corresponds to the exact normalization of the large component of the relativistic 4-component wave function.

In Eqs. 1 and 4, $\mathbf{S}$, $\mathbf{T}$, and $\mathbf{V}$ are the matrices of the non-relativistic overlap, kinetic energy, and potential energy operators, whereas $\mathbf{W}$ is the matrix of the operator $(1/4m^2c^2)\boldsymbol{\sigma}\cdot\mathbf{p}V(\mathbf{r})\boldsymbol{\sigma}\cdot\mathbf{p}$ $((1/4m^2c^2)\nabla\mathrm{V}(\mathbf{r})\cdot\nabla$ in scalar relativistic approximation) in the basis of the atomic orbitals $\chi_\mu(\mathbf{r})$ [31]. Note that, with the use of bare nuclear potential $V(\mathbf{r})$, $\mathbf{W}$ is a negative definite matrix. The scalar relativistic approximation is used throughout this article with the velocity of light $c = 137.035999679$ [59].

The NESC Hamiltonian $\tilde{\mathbf{L}}$ is obtained iteratively by solving the following system of equations [31, 38]

$$\tilde{\mathbf{L}} = \mathbf{TU} + \mathbf{U}^\dagger\mathbf{T} - \mathbf{U}^\dagger(\mathbf{T}-\mathbf{W})\mathbf{U} + \mathbf{V} \quad (5)$$

$$\mathbf{U} = \mathbf{T}^{-1}(\mathbf{S}\tilde{\mathbf{S}}^{-1}\tilde{\mathbf{L}} - \mathbf{V}). \quad (6)$$

It is convenient to start the iterative solution of Eqs. 5 and 6 from the solutions of the matrix IORA equation (7) [35],

$$\tilde{\mathbf{L}}^{\mathrm{IORA}}\mathbf{A}^{\mathrm{IORA}} = \tilde{\mathbf{S}}^{\mathrm{IORA}}\mathbf{A}^{\mathrm{IORA}}\boldsymbol{\varepsilon}^{\mathrm{IORA}} \quad (7)$$

where the Hamiltonian $\mathbf{L}^{\mathrm{IORA}}$ and the metric $\mathbf{S}^{\mathrm{IORA}}$ are obtained using Eq. 8 in Eqs. 4 and 5 [30].

$$\mathbf{U}^{\mathrm{IORA}} = (\mathbf{T}-\mathbf{W})^{-1}\mathbf{T} \quad (8)$$

Because $\mathbf{W}$ is a negative definite matrix, Eq. 8 will not diverge.

As was observed in Ref. 38, the aforementioned iterative solution of Eqs. 5 and 6 may become unstable with the use of local atom-centered basis sets which include very tight functions (e.g. Gaussian-type functions with very large exponents). The origin of the instability can be traced back to the occurrence of large positive eigenvalues of the NESC Hamiltonian (5), $\varepsilon_k > > 2\mathrm{mc}^2$ [38]. For the purpose of demonstrating this, we transform Eq. 6 as in Eq. 9,

$$\mathbf{U} = \mathbf{T}^{-1}\left((\mathbf{I} + \frac{1}{2\mathrm{mc}^2}\mathbf{U}^\dagger\mathbf{TUS}^{-1})^{-1}\tilde{\mathbf{L}} - \mathbf{V}\right) \quad (9)$$

through Eq. 4 and the formula

$$\mathbf{S}\tilde{\mathbf{S}}^{-1} = (\tilde{\mathbf{S}}\mathbf{S}^{-1})^{-1} = (\mathbf{I} + \frac{1}{2\mathrm{mc}^2}\mathbf{U}^\dagger\mathbf{TUS}^{-1})^{-1} \quad (10)$$

where $\mathbf{I}$ is a unit matrix. Using the identity $(\mathbf{I}+\mathbf{A})^{-1} = \mathbf{I} - \mathbf{A}\,(\mathbf{I}+\mathbf{A})^{-1} = \mathbf{I} - (\mathbf{I}+\mathbf{A})^{-1}\,\mathbf{A}$ [60] and replacing $\tilde{\mathbf{L}}$ by Eqs. 5 and 9 can be transformed to Eq. 11,

$$\mathbf{U} = \mathbf{T}^{-1}\Bigg(\mathbf{TU} + \mathbf{U}^\dagger\mathbf{T} - \mathbf{U}^\dagger(\mathbf{T}-\mathbf{W})\mathbf{U}. - \frac{1}{2\mathrm{mc}^2}\mathbf{U}^\dagger\mathbf{TUS}^{-1}\left(\mathbf{I} + \frac{1}{2\mathrm{mc}^2}\mathbf{U}^\dagger\mathbf{TUS}^{-1}\right)^{-1}\tilde{\mathbf{L}}\Bigg) \quad (11)$$

from which one can obtain Eq. 12:

$$\mathbf{U} = \mathbf{U}^{\mathrm{IORA}} - \frac{1}{2\mathrm{mc}^2}\mathbf{U}^{\mathrm{IORA}}\mathbf{U}\tilde{\mathbf{S}}^{-1}\tilde{\mathbf{L}}. \quad (12)$$

Iterating Eq. 12 and using eigenvalues and eigenvectors of NESC Eq. 3 one can derive

$$\begin{aligned}\mathbf{U} &= \mathbf{U}^{\mathrm{IORA}} + \mathbf{U}^{\mathrm{IORA}}\mathbf{UA}\left(-\frac{\boldsymbol{\varepsilon}}{2mc^2}\right)\mathbf{A}^\dagger\tilde{\mathbf{S}}\\ &= \mathbf{U}^{\mathrm{IORA}} + \mathbf{U}^{\mathrm{IORA}}\left(\mathbf{U}^{\mathrm{IORA}} + \mathbf{U}^{\mathrm{IORA}}\mathbf{UA}\left(-\frac{\boldsymbol{\varepsilon}}{2mc^2}\right)\mathbf{A}^\dagger\tilde{\mathbf{S}}\right)\mathbf{A} \times \left(-\frac{\boldsymbol{\varepsilon}}{2mc^2}\right)\mathbf{A}^\dagger\tilde{\mathbf{S}}\\ &= \mathbf{U}^{\mathrm{IORA}} + \left(\mathbf{U}^{\mathrm{IORA}}\right)^2\mathbf{A}\left(-\frac{\boldsymbol{\varepsilon}}{2mc^2}\right)\mathbf{A}^\dagger\tilde{\mathbf{S}} + \left(\mathbf{U}^{\mathrm{IORA}}\right)^2\mathbf{UA}\left(-\frac{\boldsymbol{\varepsilon}}{2mc^2}\right)^2\mathbf{A}^\dagger\tilde{\mathbf{S}}\\ &= \sum_{k=0}^{2}\left(\mathbf{U}^{\mathrm{IORA}}\right)^{k+1}\mathbf{A}\left(-\frac{\boldsymbol{\varepsilon}}{2mc^2}\right)^k\mathbf{A}^\dagger\tilde{\mathbf{S}} + \left(\mathbf{U}^{\mathrm{IORA}}\right)^3\mathbf{UA}\left(-\frac{\boldsymbol{\varepsilon}}{2mc^2}\right)^3\mathbf{A}^\dagger\tilde{\mathbf{S}}\\ &= \sum_{k=0}^{\infty}\left(\mathbf{U}^{\mathrm{IORA}}\right)^{k+1}\mathbf{A}\left(-\frac{\boldsymbol{\varepsilon}}{2mc^2}\right)^k\mathbf{A}^\dagger\tilde{\mathbf{S}}\end{aligned} \quad (13)$$

from which it is obvious that the convergence of the derived expansion is stable and monotonic for negative

eigenvalues $-2mc^2 < \varepsilon_k < 0$. However, occurrence of the positive eigenvalues ε_k leads to oscillating convergence and, for eigenvalues $\varepsilon_k > 2mc^2$, the expansion (12) may become divergent.

In this work, we will investigate and compare four different procedures of solving the NESC equations. These include iterative procedures suggested in the literature or developed in this work as well as the one-step method originally suggested by Dyall [31] but only recently realized in the IOTC [44], X2C [52], and the IOTC/X2C methods [49]. Primary objective of this comparison is a way of rapidly determining the matrix **U** in those cases where repeated calculation of the NESC energy, NESC gradient, and NESC Hessian is required as for example in a reaction path following algorithm of URVA (see above) [57]. A priori one could assume that the latter algorithm should be preferred; however, we will show in the following that iterative algorithms as used by Filatov and Dyall [38] (the so-called damping method), the Newton-Raphson method investigated by Liu and Kutzelnigg [52] or a new procedure, which we have coined the iterative TU method, still have their merits.

Damping method. Filatov and Dyall [38] suggested to improve the convergence of the iterative solution of the NESC equations by modifying Eq. 6 as in Eq. 14

$$\mathbf{U} = \mathbf{T}^{-1}(\mathbf{SAdA}^{\dagger}\tilde{\mathbf{L}} - \mathbf{V}) \tag{14}$$

and introducing a diagonal matrix **d** of damping coefficients, see Eq. 15,

$$d_k = \begin{cases} 1, & \varepsilon_k \leq 0 \\ (1 + \varepsilon_k/2mc^2), & \varepsilon_k > 0 \end{cases} \tag{15}$$

which damps contributions of those eigenvectors corresponding to the very large positive eigenvalues ε_k of the NESC Hamiltonian (2). Although the approach described guarantees quick and stable convergence for the negative eigenvalues ε_k, the positive eigenvalues may remain unconverged. Consequently in some cases it occurs that both the NESC eigenvalues and the total energy become dependent on the damping coefficients. For example, we observed that for Hg(^1S) described with standard basis sets (Sect. 3), deviations in the total energy are as large as 0.1 Hartree per iteration step. It is therefore desirable to obtain accurate solutions of Eqs. 3–6 without imposing restrictions on the eigenvalue spectrum.

Newton-Raphson method Liu and Kutzelnigg [52] suggested a Newton-Raphson procedure to solve the quasi-relativistic equation. For the NESC method, this implies the following steps. If Eq. 12 is written for the eigenvector a_μ of **A** of Eq. 3, one obtains

$$\mathbf{U}\mathbf{a}_\mu = \left((\mathbf{U}^{\mathrm{IORA}})^{-1} + \frac{\varepsilon_\mu}{2mc^2}\right)^{-1}\mathbf{a}_\mu = \mathbf{b}_\mu. \tag{16}$$

All eigenvectors of iteration step n can be collected in $\mathbf{A}^{(n)}$ to obtain **U** of step $n + 1$:

$$\mathbf{U}^{(n+1)} = \mathbf{B}^{(n)}\mathbf{A}^{(n)\dagger}\tilde{\mathbf{S}}^{(n)} \tag{17}$$

with the help of the matrix identity

$$\tilde{\mathbf{S}} = \left(\mathbf{A}\mathbf{A}^{\dagger}\right)^{-1}. \tag{18}$$

An iterative scheme as such does not guarantee convergence of **U** and therefore a Newton-Raphson approach is applied. With the help of Eq. 19 (which follows from Eq. 12 using the identity $\mathbf{S}^{-1}(\mathbf{TU} + \mathbf{V}) = \tilde{\mathbf{S}}^{-1}\tilde{\mathbf{L}}$ [55])

$$\mathbf{U} = \mathbf{U}^{\mathrm{IORA}}\left[\mathbf{I} - \frac{1}{2mc^2}\mathbf{U}\mathbf{S}^{-1}(\mathbf{TU} + \mathbf{V})\right]. \tag{19}$$

An error matrix **G** = **G**(**U**) is defined

$$\mathbf{G}(\mathbf{U}) = \mathbf{I} - \frac{1}{2mc^2}\mathbf{U}\mathbf{S}^{-1}(\mathbf{TU} + \mathbf{V}) - (\mathbf{U}^{\mathrm{IORA}})^{-1}\mathbf{U} \approx \mathbf{0}. \tag{20}$$

Replacing **U** by $\mathbf{U} + \mathbf{\Delta}$ and neglecting the quadratic term of **Δ**, one obtains

$$\begin{aligned}\mathbf{G}(\mathbf{U} + \Delta) = \mathbf{G}(\mathbf{U}) &- \frac{1}{2mc^2}\left[\mathbf{\Delta}\mathbf{S}^{-1}(\mathbf{TU} + \mathbf{V}) + \mathbf{U}\mathbf{S}^{-1}\mathbf{T}\Delta\right] \\ &- (\mathbf{U}^{\mathrm{IORA}})^{-1}\mathbf{\Delta} \\ &\approx \mathbf{0}.\end{aligned} \tag{21}$$

Inserting Eq. 6 into Eq. 21 leads to

$$\mathbf{G}(\mathbf{U}) = \frac{1}{2mc^2}\left(\mathbf{\Delta}\tilde{\mathbf{S}}^{-1}\tilde{\mathbf{L}} + \mathbf{U}\mathbf{S}^{-1}\mathbf{T}\Delta\right) + (\mathbf{U}^{\mathrm{IORA}})^{-1}\mathbf{\Delta}. \tag{22}$$

If one applies Eq. 22 to eigenvector a_μ of Eq. 3 and the matrix identity of Eq. 18 again, Eqs. 23 and 24 result:

$$\begin{aligned}\mathbf{\Delta}\mathbf{a}_\mu &= \left((\mathbf{U}_{\mathrm{IORA}})^{-1} + \frac{1}{2mc^2}\mathbf{U}\mathbf{S}^{-1}\mathbf{T} + \frac{\varepsilon_\mu}{2mc^2}\mathbf{I}\right)^{-1}\mathbf{G}(\mathbf{U})\mathbf{a}_\mu \\ &= \mathbf{q}_\mu\end{aligned} \tag{23}$$

$$\mathbf{\Delta}^{(n+1)} = \mathbf{Q}^{(n)}\mathbf{A}^{(n)\dagger}\tilde{\mathbf{S}}^{(n)}. \tag{24}$$

Hence, the final **U** matrix in the $(n + 1)$-th iteration is given by

$$\mathbf{U}_{final}^{(n+1)} = \mathbf{U}^{(n+1)} + \mathbf{\Delta}^{(n+1)} \tag{25}$$

which then is used to update $\tilde{\mathbf{S}}$ and $\tilde{\mathbf{L}}$ by Eqs. 4 and 5.

This approach, called by Liu and Kutzelnigg the refined linear iteration method (Eqs. 16–18), combined with a Newton-Raphson approach (Eqs. 19–25) [52]) leads to reliable eigenvalues, however implies also a substantial computational overhead because in each iteration there are about $2 \times M$ (M number of basis functions) matrix

inversions and multiplications to be performed in Eqs. 16 and 23. Liu and Kutzelnigg also suggested some simple linear iteration methods that are computationally much cheaper (reduction of computational cost by about one half), however found that these approaches diverge for large atomic numbers Z when using large basis sets [52]. We found that this problem can be cured. It is advisable to calculate matrix **U** on the r.h.s of Eq. 12 according to

$$\mathbf{U}^{(n+1)} = 2mc^2\left(\mathbf{I} - \left(\mathbf{U}^{\mathrm{IORA}}\right)^{-1}\mathbf{U}^{(n)}\right)\left(\tilde{\mathbf{L}}^{(n)}\right)^{-1}\tilde{\mathbf{S}}^{(n)}. \qquad (26)$$

If $\mathbf{U}^{\mathrm{IORA}}$ is used as the initial **U**, Eq. 26 leads to a zero matrix in the first iteration. In this case, the **Δ** matrix from Eq. 24 is identical to the **U** matrix of Eq. 17. Therefore, the zero matrix in the first iteration does not affect the convergence.

An iterative scheme based on Eq. 26 performs similar to an approach based on Eq. 17, however it reduces computational costs substantially. When using basis functions with very large exponents, Eq. 26 leads to equally fast or even faster convergence than Eq. 17. Therefore, we have carried out all Newton-Raphson calculations utilizing Eq. 26.

One-step method The one-step method was first suggested by Dyall [31] and has been studied by Liu and Kutzelnigg [52], Iliaš and Saue [49], and Kedziera and Barysz [44]. The method is based on the fact that Eq. 19 can be cast in the form

$$\mathbf{U}\left(\frac{1}{2mc^2}\mathbf{S}^{-1}\mathbf{T}\right)\mathbf{U} + \left(\mathbf{U}^{\mathrm{IORA}}\right)^{-1}\mathbf{U} + \mathbf{U}\left(\frac{1}{2mc^2}\mathbf{S}^{-1}\mathbf{V}\right) - \mathbf{I} = \mathbf{0} \qquad (27)$$

which corresponds to a non-symmetric algebraic Riccati equation [61]:

$$\mathbf{U}\boldsymbol{\alpha}\mathbf{U} + \boldsymbol{\beta}\mathbf{U} + \mathbf{U}\boldsymbol{\gamma} + \boldsymbol{\delta} = \mathbf{0} \qquad (28)$$

where **α**, **β**, **γ**, and **δ** are known matrices. Various algorithms are known to determine the unknown matrix **U** in the Riccati equation [61]. One way of solving it implies the transformation of the M-dimensional quadratic Eq. 28 into a 2M-dimensional linear matrix equation [62], which corresponds to the Dirac equation (1) in the current case. Solving Eq. 1 by diagonalization provides all needed eigenvalues and eigenvectors. Then, the matrix **U** is directly calculated with the help of Eq. 2. Subsequently, the relativistic matrices $\tilde{\mathbf{S}}$ and $\tilde{\mathbf{L}}$ can be obtained from Eqs. 4 and 5.

In connection with the one-step method, it was pointed out in [52] that for finite basis sets negative-energy (positronic) eigenvalues, significantly above the limit $-2mc^2$, might be obtained thus leading to an inverse variational collapse (IVC). Accordingly, the total energy is no longer reliable. We have found that this problem no longer occurs when using the one-step method in connection with the modified Dirac equation (1). Even for extremely steep basis functions with exponents up to a magnitude of 10^{22} (normally not needed when working with a finite nucleus model), IVC problems were not observed when applying double numeric precision in the calculations. However, when carrying out the same calculations with the program DIRAC [63] which is based on the original Dirac equation, IVC problems already occur for basis sets with modestly steep basis functions ($\alpha \approx 10^{12}$, see application section). There are indications in the literature [13, 64] that another way of solving IVC problems is given by employing quadruple rather than double precision in the calculations. This solution, however, makes calculations expensive.

Iterative TU method From a computational point of view, solution of Eqs. 5 and 6 represents a nonlinear problem that can be solved with the use of a fixed-point iteration [65]. Indeed, Eq. 6 can be written in the form of a fixed-point problem $\mathbf{U} = \mathbf{F}(\mathbf{U})$, which can be solved as

$$\mathbf{U}^{(n)} = \mathbf{F}(\mathbf{U}^{(n-1)}) \qquad (29)$$

starting from a suitable guess $\mathbf{U}^{(0)}$. This procedure converges provided that the norm of the Jacobian matrix $\mathbf{J_F} = \partial\mathbf{F}(\mathbf{U}) \,/\, \partial\mathbf{U}$ satisfies the inequality $||\mathbf{J_F}|| < 1$ at the solution [65]. As is obvious from Eqs. 12 and 13, the latter condition may not always be satisfied, which leads to the lack of convergence of a fixed-point iteration for this equation. This problem can be bypassed with the use of the Newton-Raphson method (see above), which explicitly uses the Jacobian matrix of the function **F**(**U**) [65].

Alternatively, a much simpler solution can be obtained with the use of a damped fixed-point iteration technique often employed to solve stiff initial value problems [66]. If the direct fixed-point iteration of Eq. 29 does not converge, one can introduce a certain amount of damping to stabilize the iteration:

$$\mathbf{U}^{(n)} = \mathbf{F}(\mathbf{U}^{(n-1)}) - \alpha\left(\mathbf{F}(\mathbf{U}^{(n-1)}) - \mathbf{U}^{(n-1)}\right). \qquad (30)$$

Even in the simplest form, with a fixed damping parameter α, the use of a damped fixed-point iteration method leads to convergence of the NESC equations (4) and (5). In view of Eq. 11, the iterations are preferentially carried out for matrix product **TU** rather than matrix **U** itself and after convergence **U** is calculated with the help of the known **T** ("Iterative TU" method).

For the purpose of reducing the number of algebraic operations during the iterations, it is convenient to rewrite Eqs. 4, 5, and 6 as

$$\tilde{\mathbf{L}} = \mathbf{Z} + \mathbf{Z}^{\dagger} - \mathbf{Z}^{\dagger}(\mathbf{T}^{-1} - \mathbf{T}^{-1}\mathbf{W}\mathbf{T}^{-1})\mathbf{Z} + \mathbf{V} \qquad (31)$$

$$\mathbf{Z} = \mathbf{S}\tilde{\mathbf{S}}^{-1}\tilde{\mathbf{L}} - \mathbf{V} \qquad (32)$$

$$\tilde{\mathbf{S}} = \mathbf{S} + \frac{1}{2mc^2}\mathbf{Z}^{\dagger}\mathbf{T}^{-1}\mathbf{Z} \tag{33}$$

where $\mathbf{Z} = \mathbf{TU}$. Convergence is monitored by comparing the absolute differences in the diagonal elements of the NESC Hamiltonian (4) or (30) from successive iterations.

Comparison of methods to determine U. In view of the stability problems mentioned by Liu and Kutzelnigg [52] in connection with the one-step method, the Newton-Raphson approach has some justification, especially if the number of basis functions is small, e.g., when working with exponential functions. However, once this problem is solved there is no longer any reason to carry out the Newton-Raphson method, which is no longer competitive compared to the timings of the single-step method (see below and Fig. 1). The disadvantage of the damping method has been outlined above, and we do not recommend use of this method. Instead, we suggest two alternatives: (i) In case of single-energy calculations, the one-step method is preferable as long as one can guarantee the accuracy of the diagonalization. (ii) For repeated evaluations of the matrix **U** as required in a geometry optimization [56] or a reaction path calculation, it is more efficient to take an alternative approach: The first calculation is carried out using the one-step method. In all the subsequent calculations, the iterative TU algorithm is used, because in this situation a reasonable guess of matrix **U** is available from the previous calculation thus guaranteeing a rapid convergence in just a few iteration steps.

The TU method requires 5 matrix multiplications and one inversion leading in total to $6M^3$ floating point operations (flops) per iteration. Solving the generalized symmetric eigenvalue problem $\mathbf{Ac} = \mathbf{Bc}\boldsymbol{\lambda}$ for matrices **A** and **B** requires, in view of the dimension 2M, approximately $8 \times 18/3 \times M^3 = 48\,M^3$ flops, i.e., the TU method performs better if it converges in less than 8 iteration steps. This assessment is supported by the geometry optimizations we have carried out so far. Application of the TU algorithm reveals also that it is reliable for common basis sets (e.g., the SARC basis sets of Neese et al. [67] or the relativistic basis sets of Dyall [68, 69]), which do not possess functions with an exponent $> 10^9$. It is noteworthy that as long as a finite nucleus model is used, steeper basis functions are hardly needed.

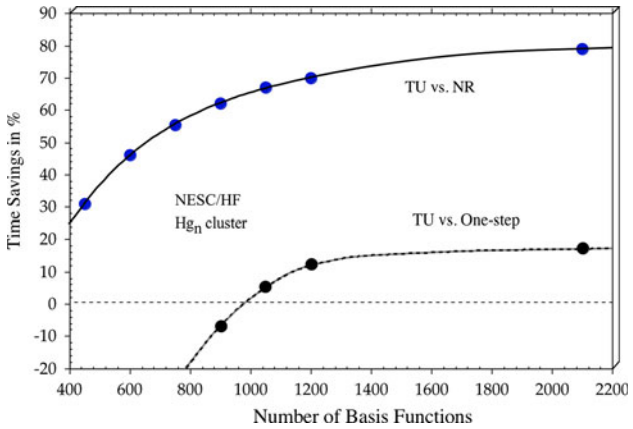

Fig. 1 Time savings achieved with the iterative TU method relative to the Newton-Raphson method (*blue points*) and the one-step method (*black dots*) in NESC/HF calculations for linear Hg_n clusters with increasing *n* and increasing number of basis functions. Positive values indicate time savings obtained with the first method relative to the second method. The *dashed zero line* is included to indicate when the TU method becomes faster than the NR or one-step method (compare with Table 2)

Application to many-electron systems. NESC Eq. 3 provides the exact electronic solutions of the 4-component one-electron problem. For the purpose of utilizing these solutions and the pertinent Hamiltonian operator (4) for the calculation of a many-electron system, one can employ the one-electron approximation as suggested by Dyall [32, 70]. Within this approximation, the one-electron NESC Hamiltonian is renormalized on the non-relativistic metric [32, 70]

$$\mathbf{H}_{1-e} = \mathbf{G}^{\dagger}\tilde{\mathbf{L}}\mathbf{G} \tag{34}$$

so that $\mathbf{H}_{1\text{-}e}$ can be applied in connection with the non-relativistic Hartree-Fock or Kohn-Sham equations. Dyall used Eq. 35 for the renormalization [32, 70],

$$\mathbf{G} = \tilde{\mathbf{S}}^{-1/2}\mathbf{S}^{1/2} \tag{35}$$

which, however, suffers from an error due to inappropriate treatment of the picture change (PC). A PC-corrected renormalization was suggested by Liu and Peng [53],

$$\mathbf{G} = \mathbf{S}^{-1/2}\left(\mathbf{S}^{1/2}\tilde{\mathbf{S}}^{-1}\mathbf{S}^{1/2}\right)^{1/2}\mathbf{S}^{1/2}. \tag{36}$$

The energy difference between the two renormalization methods cannot be neglected except for one-electron systems [53]. Note that the matrices for the uncontracted basis set are used in Eqs. 35 and 36 [32, 70]. The total electronic energy at the level of the independent-particle, self-consistent-field approximation is then given by Eq. 37,

$$E = tr\mathbf{P}\mathbf{H}_{1-e} + \frac{1}{2}tr\mathbf{P}(\mathbf{J} - \mathbf{K}) \tag{37}$$

where **J** and **K** are the Coulomb and the exchange parts of the Fock matrix and **P** is the density matrix calculated as $\mathbf{P} = \mathbf{CnC}^{\dagger}$ (**C** collects the eigenvectors of the Fock matrix and **n** is the diagonal matrix of the orbital occupation numbers). Within the one-electron approximation, the potential energy of the electron-nuclear attraction is used when calculating the **V** and **W** matrices in Eqs. 5, 6, 14, and 8 [32].

As has been shown by Dyall [32, 70], the one-electron approximation deviates from the exact FW-transformed

relativistic equations by neglecting the renormalized two-electron Darwin term, which originates from the commutator of the electron–electron interaction operator and the relativistic transformation operator. Within the one-electron approximation, the spin orbit interaction can be suitably included utilizing the atomic mean field integrals (AMFI) approach, which is commonly employed in connection with the DKH method [71].

First-Diagonalize-then-Contract. It was tacitly assumed so far that the NESC equations are solved in a sufficiently large basis set of primitive functions. Indeed, using such a basis set, one can reproduce the exact analytic solutions of the Dirac equation for one electron with a sufficiently high accuracy [31, 38, 70]. In the case of many-electron calculations, however, such an approach has the disadvantage that a large number of two-electron integrals need to be evaluated, which may lead to unacceptably high computational cost. It is therefore desirable to employ contracted basis sets in connection with the many-electron calculations. Dyall has considered a contraction scheme, in which the relativistic transformation (1) is folded into the contraction coefficients [70]. This, however, leads to the necessity of developing three sets of contracted basis functions [70] and to considerable difficulties with devising segmented contraction of the basis set [32]. For the purpose of bypassing these difficulties, we employ the following strategy: The NESC one-electron equations are solved in the basis set of the primitive basis functions and the resulting renormalized one-electron Hamiltonian (33) is converted to a contracted basis set. This strategy has the advantage that only one set of contraction coefficients is needed and that the use of both generally contracted basis sets as well as basis sets with segmented contraction becomes straightforward. Furthermore, using this "First-Diagonalize-then-Contract" approach, the atomic many-electron total energies obtained with a contracted basis set are within less than 1 Hartree from the energies obtained when employing the corresponding uncontracted basis set. Therefore, we have used the "First-Diagonalize-then-Contract" strategy throughout this work. In this connection, it is useful to mention that the latter strategy is in the same spirit as the computational approach employed by the DKH method when transforming to momentum space. The transformation is carried out in the uncontracted basis set whereas the contraction coefficients are applied to the final quasi-relativistic Hamiltonian [72].

3 Computational techniques

The algorithms described above have been programmed within the COLOGNE2010 program package [73]. The four-component Dirac–Hartree–Fock (4c-DHF) calculations, with RKB or UKB (unrestricted kinetic balance) conditions to construct the small-component basis set, were performed using the DIRAC program package [63]. For the IOTC [42–44, 47] and relativistic elimination of small component (RESC) [74] calculations, the GAMESS program packages [75] were used. The Dirac, NESC, and all other quasi-relativistic calculations for hydrogen-like ions were carried out with a universal basis set of 50 primitive s-type Gaussian functions taken from Wolf et al. [14] where the exponents of the s-functions are defined by $\alpha_i = \exp[-3.84 + (i-1)0.72]$, $i = 1, 2, 3, \ldots, 50$. In order to compare with the results published by Wolf et al. [14], Reiher and Wolf [17], or Peng and Hirao [64], a previously used value of $c = 1/\alpha = 137.0359895$ had to be used for the calculations listed in Table 1. All other calculations were carried out with the value of c given in Sect. 2 [59].

In connection with the NESC/HF calculations of Table 2, the (22s15p11d6f) set of primitive basis functions of the SARC basis library [67] was taken and contracted according to Hg(^1S) calculations at the HF level. For the NESC/finite nucleus calculations [3, 76], the core functions were re-contracted and two diffuse *f*-functions were deleted thus obtaining a (22s15p11d4f)/[17s11p8d1f] basis set with the pattern {61111111111111111/5111111111/41111111/4}. Spherical basis functions were used throughout, which leads to 150 primitive basis functions for each Hg atom.

In the case of the HgX calculations of Table 3, bond lengths were obtained at the NESC/CCSD level of theory (F, Cl, Br, I: 2.024, 2.402, 2.546, 2.709 Å) utilizing a segmented contracted basis set for Hg of the (22s19p12d9f) / [15s13p8d5f] type [77]. For F, Cl, and Br, Dyall's Dirac-contracted cc-pVTZ(fi/sf/fw) basis with the diffuse functions from the nonrelativistic aug-cc-pVTZ basis was used [78]. A (22s15p11d6f) SARC basis set was also taken for Tl and adjusted to finite nucleus calculations in the same way as the corresponding Hg basis. The Tl basis set was augmented with 3g2h1i polarization functions [79]. An all-electron def2-QZVPP basis set [78] was used for F, Cl, and Br in TlX. Again, the core functions were re-contracted for the finite nucleus calculations as described above. The relativistic def2-TZVPP basis set of I [67], also re-contracted, was used for both HgI and TlI. The NESC/DFT calculations were performed with the PBE0 functional [80, 81] and NESC/PBE0 bond lengths of 2.096, 2.504, 2.642, and 2.842 Å (TlF to TlI).

4 Results and discussions

In Table 1, quasi-relativistic Hartree-Fock (HF) energies of hydrogen-like multiply charged cations with atomic numbers Z = 20, 40, …, 120 are compared with exact 4c-DHF (Dirac–HF) calculations. 4c-DHF atomic energies equivalent to the basis set limit for the hydrogen-like cations can be obtained from

Table 1 Ground state energies (in Hartree) of hydrogen-like ions obtained with different 4c-, 2c-, and 1c-relativistic methods

Method	$Z = 20$	$Z = 40$	$Z = 60$	$Z = 80$	$Z = 100$	$Z = 120$
Point charge nuclear model with 50 s-functions[a]						
Dirac equation	−201.076523	−817.807498	−1895.68236	−3532.19215	−5939.19538	−9710.78352
4c-DHF(RKB) [13]	−201.07652	−817.80749	−1895.68234	−3532.19213	−5939.19514	−9710.71531
4c-DHF(UKB) [tw]	−201.076522	−817.807491	−1895.68234	−3532.19213	−5939.19514	−9710.71531
NESC [tw]	−201.076522	−817.807491	−1895.68234	−3532.19213	−5939.19514	−9710.71531
Other methods						
RESC[b]	−201.170853	−819.576517	−1904.19372	−3553.51917	−5954.76495	−9501.18126
ZORA [30]	−202.158829	−836.011368	−1996.45087	−3898.86916	−7054.8079	−13096.9617
IORA [30]	−201.082194	−818.171957	−1899.90000	−3536.90102	−6042.5850	−10089.4142
NESC-SORA [30]	−201.076522	−817.807633	−1895.68972	−3532.31224	−5940.2749	−9718.0099
DKH2 [17]	−201.072540	−817.615780	−1893.89769	−3523.32490	−5906.1919	−9594.1000
DKH3 [17]	−201.076662	−817.820117	−1895.84407	−3533.11958	−5942.3695	−9712.9340
DKH14 [17]	−201.076523	−817.807497	−1895.68235	−3532.19184	−5939.1821	−9710.2510
DKH_n, $(n > 20)$ [64]				−3532.19213		
Point charge nuclear model with 40 s-functions[c]						
NESC [tw]	−201.076522	−817.807490	−1895.68231	−3532.19120	−5939.16486	−9708.57973
4c-DHF(RKB) [tw]	$<1 \times 10^{-8}$	$<1 \times 10^{-8}$	$<1 \times 10^{-8}$	4×10^{-8}	5×10^{-8}	6×10^{-8}
4c-DHF(UKB) [tw]	$<1 \times 10^{-8}$	$<1 \times 10^{-8}$	$<1 \times 10^{-8}$	$<1 \times 10^{-8}$	$<1 \times 10^{-8}$	$<1 \times 10^{-8}$
IOTC/X2C [tw]	$<1 \times 10^{-8}$	$<1 \times 10^{-8}$	$<1 \times 10^{-8}$	3×10^{-8}	5×10^{-8}	6×10^{-8}
IOTC [tw]	1×10^{-6}	2×10^{-7}	5×10^{-8}	2×10^{-7}	9×10^{-7}	3×10^{-6}
Finite nuclear model with 50 s-functions[d]						
4c-DHF(UKB) [tw]	−201.076001	−817.788172	−1895.45071	−3530.19419	−5922.78995	−9545.87512
NESC [tw]	−201.076001	−817.788172	−1895.45071	−3530.19419	−5922.78995	−9545.87512

[a] Because of inverse variational collapse, the 4c-DHF(RKB), IOTC/X2C, and IOTC values obtained this work [tw] are not listed

[b] For Z = 60–120, only the first 41 s-functions were used because of variational collapse

[c] Energy differences between NESC and other methods are given

[d] Mass number of isotope was taken from Ref. [76]. For Z = 120, mass number = 2.556*Z = 306.72. For Z = 119–137, there are a regular and an irregular solutions. The potential energy matrix **V** is checked to distinguish between regular (finite) or irregular solution (infinite values of **V**). See Ref. [95, p. 274]. The 4c-DHF(RKB) results are not shown because of inverse variational collapse.

$$E(1s_{1/2}) = mc^2\left(\sqrt{1-(Z\alpha)^2}-1\right). \quad (38)$$

The finite basis set 4c-DHF energies are 0.01 up to 1 mHartree higher in energy for Z ≤ 100 and almost 70 mhartree in the case of Z = 120. In Table 1, RKB [33, 34] and UKB 4c-DHF energies [13] are listed where the RKB (UKB) procedure has the purpose of avoiding a catastrophic variational collapse caused by an inappropriate description of the small component and by this a serious underestimation of the kinetic energy [82–84]. Usually, UKB energies are higher than RKB energies; however, in the case of the 1-electron systems exclusively described with uncontracted s-functions for the large component, the RKB approach and the UKB approach should lead to the same energies. NESC reproduces the 4c-DHF atomic energies in all cases, which confirms that NESC is an exact quasi-relativistic method. When calculating the corresponding RKB energies with the program DIRAC [63], we ran into IVC problems, which vanished by eliminating the 10 steepest basis functions. Similar observations were made using the matrix-driven IOTC/X2C [49] in DIRAC [63] and the operator-driven IOTC methods [44] in GAMESS [75]. In Table 1, a comparison of the energies obtained with 40 s-functions is also given. As expected, the 4c-DHF(UKB), 4c-DHF(RKB), NESC, IOTC/X2C, and IOTC energies obtained differ by less than 10^{-6} Hartree, underlining that the three quasi-relativistic methods lead to exact energies.

It is well known that perturbational methods such as DKH or RA, which do not provide an upper bound to the correct DHF energy, approach the exact results in an oscillatory manner, overestimating or underestimating exact atomic energies. This is also reflected by the data in Table 1. For Z ≤ 60, DKHn atomic energies with n = 14 are close to exact values whereas for Z > 60, one has to apply DKHn with n > 20. Infinite-order DKH theory correctly reproduces NESC and DHF energies in all cases.

Table 2 Time savings obtained with the Iterative TU method relative to the Newton-Raphson method and the one-step method for NESC/HF calculations of linear Hg_n clusters

n	*M*	*E* (Hartree)	Time savings TU(I) versus NR[a] (%)	Time savings TU(O) versus one-step[a] (%)
1	150	−19618.6354121	0	
2	300	−39237.2579430	0	
3	450	−58855.8804389	31	
4	600	−78474.5031191	46	
5	750	−98093.1258063	55	−25
6	900	−117711.7485061	62	−7
7	1050	−137330.3711959	67	5
8	1200	−156948.9938766	70	12
14	2100	NESC part only	79	17

M number of basis functions. TU(I) and TU(O) denote that the initial guess for matrix **U** was obtained with the IORA (I) method and the one-step (O) method, respectively. In the latter case, the situation of a geometry optimization was simulated by calculating matrix **U** at a Hg-Hg distance 0.1 Å shifted from the target distance for which the actual calculation was carried out. For the one-step method, 1−3% of the computer time of the NR method was used. For $n = 14$, only the NESC part was calculated. All calculations were carried out using the Dyall renormalization of Eq. 35

[a] A positive (negative) value denotes time savings (losses) of the first method relative to the second method. In the case of a small M, the differences between TU(O) and one-step method were so small that a comparison was not useful

Table 3 Total energies and BDEs of HgX and TlX (X = F, Cl, Br, and I) molecules

Molecule	State	Method	Absolute E (Eq. 35)	Absolute E (Eq. 36)	BDE	BDH+ SO	Exp. BDH
HgF	$^2\Sigma^+$	NESC-CCSD(T)	−19726.5582307	−19720.0429423	33.0	32.3	32.9 [85]
HgCl	$^2\Sigma^+$	NESC-CCSD(T)	−20087.9428739	−20081.3538500	23.8	23.4	23.4 [86], 24.6 [87]
HgBr	$^2\Sigma^+$	NESC-CCSD(T)	−22231.8995139	−22224.4241374	20.0	17.5	17.2 [87], 18.4 [88]
HgI	$^2\Sigma^+$	NESC-CCSD(T)	−26740.7445756	−26732.4013087	12.9	7.6	7.8 [89], 8.1 [86], 8.9 [87]
TlF	$^1\Sigma^+$	NESC-PBE0	−20355.7541876	−20348.8772434	117.0	102.4	105.4 [90]
TlCl	$^1\Sigma^+$	NESC-PBE0	−20717.4160894	−20710.4986600	101.4	86.4	88.1 [90]
TlBr	$^1\Sigma^+$	NESC-PBE0	−22862.2828606	−22855.0357093	93.1	76.1	78.8 [90]
TlI	$^1\Sigma^+$	NESC-PBE0	−27372.1012052	−27363.2456874	83.1	61.2	63.7 [90]

Absolute energies E in Hartree, Bond Dissociation Energies (BDE), Bond Dissociation Enthalpies (BDH) + Spin-Orbit(SO) coupling corrections in kcal/mol; SO, ZPE, and thermochemical corrections of HgX and TlX were taken from Refs [90–92]. Experimental BDH (Exp. BDH) values from [85–90]. The BDE values listed in this table were calculated using the renormalization Eq. 35. The BDE values determined with Eq. 36 and including PC corrections are 0.2 (X = F, Cl, Br) or 0.1 (*X* = I) kcal/mol larger

However, it becomes also obvious that convergence of the DKHn energies to the correct result is rather slow.

Methods based on the RA converge much faster, however, largely overshoot exact results at the ZORA and IORA level where the latter is slightly better because of the infinite-order description in connection with the relativistic normalization of the wave function. Dyall and Fægri have provided arguments [3] that imply E(DHF) > E(IORA) > E(ZORA), which are confirmed by the energies of Table 1. The development of a matrix formulation for the methods based on RA by Filatov and Cremer have made it possible to consider second- and third-order IORA methods [28] and to connect the RA directly to NESC for example via the NESC-SORA (second-order regular approximation) method. NESC-SORA provides, not surprisingly, exact results for small Z whereas for larger Z its energies again overshoot exact DHF energies (Table 1).

The RESC method led to a variational collapse in the case of $Z > 60$. After eliminating the 9 steepest basis functions, RESC energies could be obtained; however, a comparison with other energy data was not possible. In all cases where a comparison is possible, the RESC energies obtained strongly overshoot exact energies.

It is well known that relativistic calculations benefit from a model of the nucleus with a finite rather than a zero radius (point charge model) [3, 76]. For example, the weak singularity of the Dirac equation at the position of the nucleus (point charge model) is avoided. The increase in energy as described by the 4c-DHF method is correctly reproduced by the NESC method (Table 1).

In summary, NESC is basically equivalent to the IOTC and IOTC/X2C methods in so far as they all lead to exact quasi-relativistic energies. Differences between these methods exist with regard to the ways of handling the calculation of **U**, the renormalization of the one-electron hamiltonian, the contraction of basis functions, etc. NESC is superior to methods based on (1) perturbation theory either with or without infinite-order schemes or (2) simplified ESC methods. NESC is exact and easier to apply than many of the methods listed in Table 1 (see also the following).

In Table 2, the performance of the Newton-Raphson method, the iterative TU, and the one-step procedure are compared for clusters of mercury atoms (Hg, ^1S) linked linearly to each other at a distance of 3Å between nearest neighbors. For Hg_n with $n = 1$, the basis set comprises 150 primitive basis functions whereas for the largest Hg_n cluster considered ($n = 14$) 2100 primitive basis functions were used (in this case, only the NESC part was calculated). Comparison of computational cost was carried out at the level of the uncontracted basis set in view of the computational strategy "First-Diagonalize-then-Contract" adopted in this work, i.e., carry out the NESC calculations for the uncontracted basis rather than the contracted one. For the Newton-Raphson method, the simple linear iterative scheme according to Eq. 26 was used because it turned out to be the least costly and at the same time the most stable one. All results obtained with the iterative TU scheme were checked against the iterative Newton-Raphson scheme, and agreement in calculated energies was up to 13 significant digits. In this set of calculations, we started from a IORA guess for matrix **U** whereas in a second set of TU calculations we simulated the situation of a geometry optimization by utilizing, as a starting guess for the TU algorithm at current geometry, the matrix **U** obtained in a calculation where the mercury positions were shifted by 0.1 Å.

Calculations revealed that, up to 300 primitive basis functions, cpu times are comparable for the Newton-Raphson and the iterative TU approach. For larger number of primitive basis functions, time savings of the iterative TU approach increase from about 30 % (450 primitives) to 80% (2100 primitives) (see Table 2; Fig. 1). These time savings are, however, much larger if the TU method starts from a better guess for the **U** matrix. In this situation, the TU approach becomes competitive with the one-step method. For large uncontracted basis sets, up to 17 % cpu time could be saved compared to the timings of the one-step method. In general, the one-step method requires only 1 to 3 % of the time required for the Newton-Raphson method and therefore the time savings may be considered as being rather small. In the situation of a reaction path analysis, 10^3 and more energy (and gradient) calculations are typically required, such that a time saving of just 10 s for a single determination of **U** leads to a time reduction of 10,000 s and more and therefore should be exploited.

In Table 3, some NESC/CCSD(T) and NESC/DFT calculations are summarized to illustrate the applicability of the algorithm described in Sect. 2. In this paper, just the bond dissociation energies (BDEs) of HgX and TlX (X = F, Cl, Br, I) molecules are discussed. Geometries and vibrational frequencies for the molecules of Table 3 have been obtained at either the NESC/CCSD or NESC/PBE0 level of theory using the same basis set as for the single point calculations. Bond dissociation enthalpies (BDH) at 298 Kelvin, which can be directly compared with experimental values [85–90], have been determined by correcting BDE values for zero-point energies, thermochemical differences between 0 and 298 Kelvin and spin-orbit (SO) coupling contributions where the latter were calculated by using SO pseudopotentials either via the state-interaction approach perturbationally or via SO-CI variationally [90–92]. In this connection, it has to be pointed out that SO-coupling corrections may become unbalanced if the one- and two-electron contributions are not both present [93].

BDH(298) values of HgX ($^2\Sigma^+$) molecules calculated at the NESC/CCSD(T) level of theory differ from experimental values on the average by 0.94 kcal/mol. If one compares the individual values, then NESC/CCSD(T) suggests for HgCl ($^2\Sigma^+$) a BDH value of 23.4 obtained by Tellinghuisen et al. [86] rather than the older value of 24.6 kcal/mol [87]. Similarly, NESC/CCSD(T) supports for HgBr the experimental value of 17.2 kcal/mol [87], and for HgI the value of 7.8 kcal/mol [89].

The same level of agreement cannot be expected for NESC/DFT although calculations have been carried out with an all-electron SARC basis augmented by 3g2h1i polarization functions. In view of a much smaller basis set truncation error at the DFT level, the purpose of including high angular momentum polarization functions was more a question of testing the methods developed rather than a question of chemical accuracy. The average deviation calculated from experimental BDH values in the case of TlX molecules is 2.9 kcal/mol where the largest deviation is found for the TlF ($^1\Sigma^+$) (3.7 kcal/mol, Table 3). Apart from this, there is a tendency of underestimating the TlX bond strength by 2–3 kcal/mol, which probably has to do with the deficiencies of the XC functional or inaccuracies of the calculated SO couplings rather than errors of the scalar relativistic effects. Thallium establishes strongly polar bonds with electronegative atoms and accordingly the bond strength should increase from the iodide to the fluoride, which is confirmed by the BDH values. SO coupling has a strong effect (15–22 kcal/mol, Table 3) on the bond strength. The inclusion of g, h, and i polarization functions leads, as expected, to only small changes in the BDE values

(<0.1 kcal/mol). Apart from this, the results prove the feasibility of using high angular momentum functions in NESC calculations.

5 Conclusions

In this article, we have presented an improved version of the NESC method: (i) Contrary to previous versions, the NESC equations are solved for the uncontracted basis set and contraction of the basis set is carried out afterward ("First-Diagonalize-then-Contract"). Using the contracted basis sets in many-electron atomic calculations, one obtains the total electronic energies in close agreement with the energies of the corresponding uncontracted basis sets. Also, generally contracted basis sets as well as basis sets with segmented contraction can be used in the calculations. (ii) Four different strategies for calculating the matrix **U** are compared. In the case of single-energy calculations, the one-step method is most efficient whereas in repeated energy calculations as required for geometry optimizations, the iterative TU algorithm leads to significant time savings compared to the one-step method. If the latter is carried out with sufficient accuracy and IVC problems are avoided as described in this work, there is no longer any need for the Newton-Raphson approach or the previously used damping method. (iii) The picture change has been correctly accounted for the NESC Hamiltonian. (iv) A finite nucleus model based on a Gaussian charge distribution has been installed. (v) NESC exactly reproduced in all cases investigated (hydrogen-like ions with $Z \leq 120$) the 4c-DHF energies and represents therefore an exact quasi-relativistic method. NESC is superior to approximate quasi-relativistic methods whereas its time requirements compare favorably with other exact quasi-relativistic methods such as the infinite-order DKH approach.

The implementation of the NESC algorithm presented in this work makes it possible to carry out accurate quasi-relativistic calculations with HF, DFT, CASCF, CASPT2, CI, many-body pertrubation theory utilizing the Møller-Plesset perturbation operator, or coupled cluster methods. NESC is generally applicable and can be included in standard quantum chemical program packages. We have presented calculations employing high angular momentum polarization functions (including g, h, and i-basis sets) to provide evidence that CBS limit energies can be obtained at NESC/CCSD(T) or any suitable level of theory. In a forthcoming paper [56], we will show that NESC can also be used for the calculation of electric response properties (dipole moment, polarizability, etc.) utilizing analytical energy derivatives. The description of magnetic response properties will require modifications of the original NESC formalism by including a magnetic field into the elimination of the small component operator [94].

Acknowledgments This work was financially supported by the National Science Foundation, Grant CHE 071893. We thank SMU for providing computational resources. MF is grateful to SMU for the invitation as a visiting professor.

References

1. Dirac PAM (1928) Proc Roy Soc Lond A 117:610
2. Dirac PAM (1929) Proc Roy Soc Lond A 123:714
3. Dyall KG, Fægri K (2007) Introduction to relativistic quantum chemistry. Oxford University Press, Oxford
4. Reiher M, Wolf A (2009) Relativistic quantum chemistry, the fundamental theory of molecular science. Wiley-VCH, Weinheim
5. Liu W (2010) Mol Phys 108:1679
6. Foldy LL, Wouthuysen SA (1950) Phys Rev 78:29
7. Douglas M, Kroll NM (1974) Ann Phys (NY) 82:89
8. Hess BA (1985) Phys Rev A 32:756
9. Hess BA (1986) Phys Rev A 33:3742
10. Jansen G, Hess BA (1989) Phys Rev A 39:6061
11. Samzow R, Hess BA, Jansen G (1992) J Chem Phys 96:1227
12. Nakajima T, Hirao K (2000) J Chem Phys 113:7786
13. van Wuellen C (2004) J Chem Phys 120:7307
14. Wolf A, Reiher M, Hess BA (2002) J Chem Phys 117:9215
15. Wolf A, Reiher M, Hess BA (2004) J Chem Phys 120:8624
16. Reiher M, Wolf A (2004) J Chem Phys 121:2037
17. Reiher M, Wolf A (2004) J Chem Phys 121:10945
18. Seino J, Uesugi W, Haeda M (2010) J Chem Phys 132:164108
19. Chang CPM, Durand M (1986) Phys Scr 34:394
20. van Lenthe E, Baerends EJ, Snijders JG (1993) J Chem Phys 99:4597
21. Dyall KG, van Lenthe E (1999) J Chem Phys 111:1366
22. van Lenthe E, Baerends EJ, Snijders JG (1994) J Chem Phys 101:9783
23. van Lenthe E, Ehlers A, Baerends EJ (1999) J Chem Phys 110:8943
24. Filatov M (2002) Chem Phys Lett 365:222
25. Filatov M, Cremer D (2003) Mol Phys 101:2295
26. Filatov M, Cremer D (2003) J Chem Phys 118:6741
27. Filatov M, Cremer D (2003) J Chem Phys 119:1412
28. Filatov M, Cremer D (2003) J Chem Phys 119:11526
29. Filatov M, Cremer D (2005) J Chem Phys 122:044104
30. Filatov M, Cremer D (2005) J Chem Phys 122:064104
31. Dyall KG (1997) J Chem Phys 106:9618
32. Dyall KG (2002) J Comp Chem. 23:786
33. Stanton RE, Havriliak S (1984) J Chem Phys 81:1910
34. Dyall KG, Fægri K (1990) Chem Phys Lett 174:25
35. Dyall KG, Enevoldsen T (1999) J Chem Phys 111:10000
36. Filatov M, Cremer D (2002) Theor Chem Acc 108:168
37. Filatov M, Cremer D (2002) Chem Phys Lett 351:259
38. Filatov M, Dyall KG (2007) Theor Chem Acc 117:333
39. Komorovsky S, Repisky M, Malkina OI, Malkin VG, Malkin I, Kaupp M (2006) J Chem Phys 124:084108
40. Peng D, Liu W, Xiao Y, Cheng L (2007) J Chem Phys 127:104106
41. Barysz M, Sadlej AJ, Snijders JG (1997) Int J Quantum Chem 65:225
42. Barysz M, Sadlej AJ (2002) J Chem Phys 116:2696
43. Kedziera D, Barysz M (2004) J Chem Phys 121:6719
44. Kedziera D, Barysz M (2004) Chem Phys Lett 521:3093
45. Kedziera D (2005) J Chem Phys 123:074109
46. Kedziera D, Barysz M (2007) Chem Phys Lett 446:176
47. Barysz M, Mentel L, Leszczynski J (2009) J Chem Phys 130:164114
48. Iliaš M, Jensen HJA, Roos BO, Urban M (2005) Chem Phys Lett 408:210

49. Iliaš M, Saue T (2007) J Chem Phys 126:064102
50. Kutzelnigg W, Liu W (2005) J Chem Phys 123:241102
51. Kutzelnigg W, Liu W (2006) Mol Phys 104:2225
52. Liu W, Kutzelnigg W (2007) J Chem Phys 126:114107
53. Liu W, Peng D (2009) J Chem Phys 131:031104
54. Kutzelnigg W, Liu W (2006) J Chem Phys 125:107102
55. Filatov M (2006) J Chem Phys 125:107101
56. Zou W, Filatov M, Cremer D (2011) J Chem Phys 134:244117
57. Cremer D, Kraka E (2010) Curr Org Chem 14:1524
58. Kraka E (1998) In: Schleyer PvR, Allinger NL, Clark T, Gasteiger J, Kollman PA, Schaefer HF III, Schreiner PR (eds) Encyclopedia of computational chemistry, vol 4. Wiley, Chichester, pp 2437
59. Gabrielse G, Hanneke D, Kinoshita T, Nio M, Odom B (2006) Phys Rev Lett 97:030802
60. Henderson HV, Searle SR (1981) SIAM Rev 23:53
61. Lancaster P, Rodman L (1995) Algebraic Riccati equations. Oxford University Press, Oxford
62. Bini DA, Meini B, Poloni F (2008) In numerical methods for structured Markov chains. In: Bini, Meini B, Ramaswami V, Remiche M-A, and Taylor P (eds) Dagstuhl seminar proceedings no. 07461, http://drops.dagstuhl.de/opus/volltexte/2008/1398, (Internationales Begegnungs- und Forschungszentrum für Informatik (IBFI), Schloss Dagstuhl, Germany)
63. Saue T,Visscher L, Jensen HJA, Bast R, Dyall KG, Ekström U, Eliav E, Enevoldsen T, Fleig T, Gomes ASP, Henriksson J, Iliaš M, Jacob CR, Knecht S, Nataraj HS, Norman P, Olsen J, Pernpointner M, Ruud K, Schimmelpfennig B, Sikkema J, Thorvaldsen A, Thyssen J, Villaume S, Yamamoto S (2010) DIRAC, a relativistic ab initio electronic structure program. Release DIRAC10 (http://dirac.chem.vu.nl, 2010)
64. Peng D, Hirao K (2009) J Chem Phys 130:044102
65. Heath MT (2002) Scientific computing: an introductory survey. McGraw-Hill, New York, pp 151–181
66. Jansson J, Logg A (2008) ACM Trans Math Softw 35:17:1
67. Pantazis DA, Chen X-Y, Landis CR, Neese F (2008) J Chem Theory Comput 4:908
68. Dyall KG (2009) J Phys Chem A 113:12638
69. Dyall KG (2011) Theor Chem Acc 129:603
70. Dyall KG (2001) J Chem Phys 115:9136
71. Schimmelpfennig B, Maron L, Wahlgren U, Teichteil C, Fagerli H, Gropen O (1998) Chem Phys Lett 286:267
72. Reiher M (2006) Theor Chem Acc 116:241
73. Kraka E, Gräfenstein J, Filatov M, Joo H, Izotov D, Gauss J, He Y, Wu A, Polo V, Olsson L, Konkoli Z, He Z, Zou W, Cremer D (2010) COLOGNE2010
74. Fedorov DG, Nakajima T, Hirao K (2001) Chem Phys Lett 335:183
75. Schmidt MW, Baldridge KK, Boatz JA, Elbert ST, Gordon MS, Jensen JH, Koseki S, Matsunaga N, Nguyen KA, Su S, Windus TL, Dupuis M, Montgomery JA (1993) J Comput Chem 14:1347
76. Visscher L, Dyall KG (1997) At Data Nucl Data Tables 67:207
77. Cremer D, Kraka E, Filatov M (2008) Chem Phys Chem 9:2510
78. Feller D (1996) J Comp Chem 17:1571
79. Peterson KA, Yousaf KE (2010) J Chem Phys 133:174116
80. Perdew JP, Burke K, Ernzerhof M (1996) Phys Rev Lett 77:3865
81. Adamo C, Barone V (1998) J Chem Phys 110:6158
82. Kim YK (1967) Phys Rev 154:17
83. Schwarz WHE, Wallmeier H (1982) Mol Phys 46:1045
84. Schwarz WHE, Wechsel-Trakowski E (1982) Chem Phys Lett 85:94
85. Chase MW (1998) J Phys Chem Ref Data Monogr 9:1
86. Tellinghuisen J, Tellinghuisen PC, Davies SA, Berwanger P, Viswanathan KS (1982) Appl Phys Lett 41:789
87. Wilcomb BE, Bernstein RB (1976) J Mol Spectrosc 62:442
88. Ullas G, Rai SB, Rai DK (1992) J Phys B At Mol Phys 25:4497
89. Salter C, Tellinghuisen PC, Ashmore JG, Tellinghuisen J (1986) J Mol Spectrosc 120:334
90. Zou W, Liu W (2009) J Comput Chem 30:524
91. Khalizov AF, Viswanathan B, Larregaray P, Ariya PA (2003) J Phys Chem A 107:6360
92. Shepler BC, Balabanov NB, Peterson KA (2005) J Phys Chem A 109:10363
93. Iliaš M, Kellö V, Visscher L, Schimmelpfennig B (2001) J Chem Phys 115:9667
94. Dyall KG (2000) Int J Quantum Chem 78:412
95. Grant IP (2007) Relativistic quantum theory of atoms and molecules, theory and computation. Springer, New York